LBL-37099
UC-414
Preprint

Lawrence Berkeley Laboratory

UNIVERSITY OF CALIFORNIA

Physics Division

Submitted to Physical Review D

Third Family Flavor Physics in an $SU(3)^3 \times SU(2)_L \times U(1)_Y$ Model

C.D. Carone and H. Murayama

May 1995

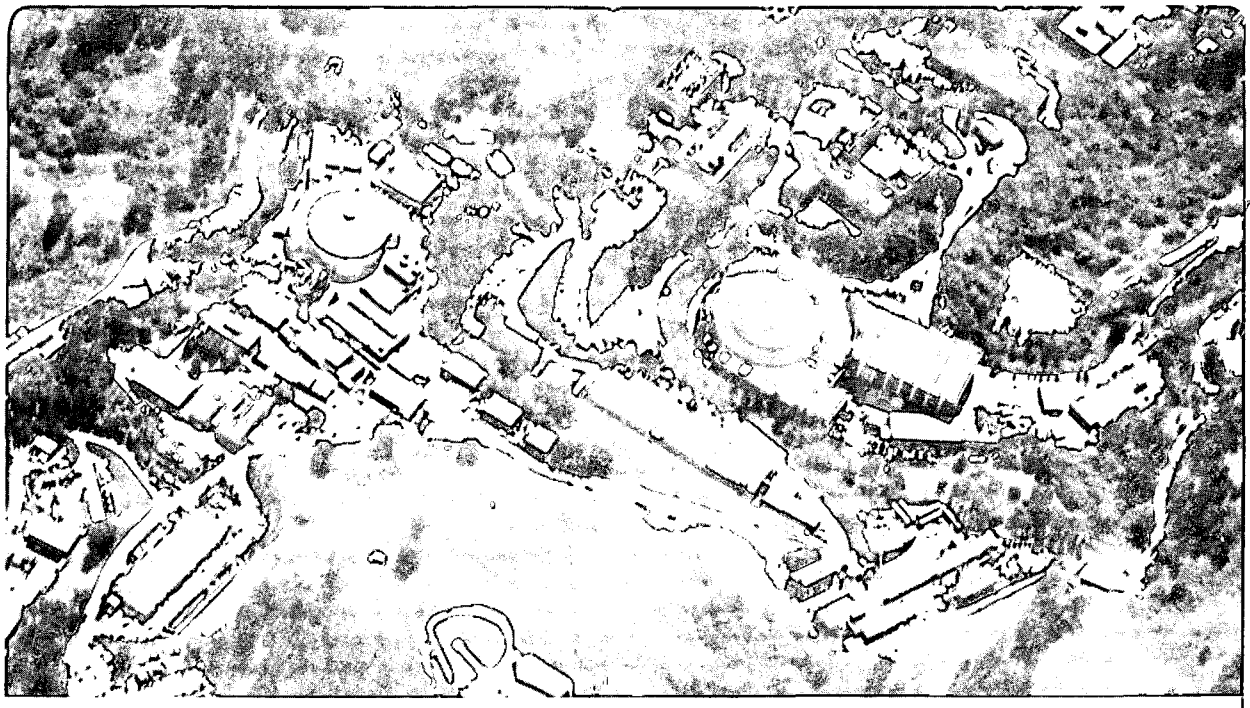

REFERENCE COPY
Does Not
Circulate
Bldg. 50 Library.
LBL-37099
Copy 1

Prepared for the U.S. Department of Energy under Contract Number DE-AC03-76SF00098

DISCLAIMER

This document was prepared as an account of work sponsored by the United States Government. While this document is believed to contain correct information, neither the United States Government nor any agency thereof, nor the Regents of the University of California, nor any of their employees, makes any warranty, express or implied, or assumes any legal responsibility for the accuracy, completeness, or usefulness of any information, apparatus, product, or process disclosed, or represents that its use would not infringe privately owned rights. Reference herein to any specific commercial product, process, or service by its trade name, trademark, manufacturer, or otherwise, does not necessarily constitute or imply its endorsement, recommendation, or favoring by the United States Government or any agency thereof, or the Regents of the University of California. The views and opinions of authors expressed herein do not necessarily state or reflect those of the United States Government or any agency thereof or the Regents of the University of California.

May 16, 1995 LBL-37099

Third family flavor physics in an $SU(3)^3 \times SU(2)_L \times U(1)_Y$ model*

Christopher D. Carone and Hitoshi Murayama†
Theoretical Physics Group
Lawrence Berkeley Laboratory
University of California
Berkeley, California 94720

Abstract

We consider a model in which each family transforms under a different SU(3) color group. The low-energy effective theory is an extension of the Standard Model, with additional color octet gauge bosons G_H with mass M that couple preferentially to the third family quarks. We show that there are two distinct regions of the model's parameter space in which we can simultaneously evade all the current experimental constraints, one with $M \approx 250$ GeV and the other with $M \gtrsim 600$ GeV. Within each allowed region, we can obtain a correction to the $Zb\bar{b}$ vertex that is consistent with the slightly high value of R_b observed at LEP. We show that there are $\Delta B = 1$ operators in our model that can suppress the B-meson semileptonic branching ratio B_{SL} and the charm multiplicity per decay n_c by enough to reconcile the spectator parton model predictions with the experimental data. In the non-supersymmetric version of our model, we can only obtain the desired corrections to R_b, B_{SL} and n_c in different regions of the allowed parameter space, while in the supersymmetric version, we can obtain all three corrections simultaneously. We also discuss a strong-coupling limit of our model in which the third-family quarks become composite.

*This work was supported by the Director, Office of Energy Research, Office of High Energy and Nuclear Physics, Division of High Energy Physics of the U.S. Department of Energy under Contract DE-AC03-76SF00098.

†On leave of absence from *Department of Physics, Tohoku University, Sendai, 980 Japan.*

1 Introduction

Despite its enormous success, the Standard Model gives us no explanation of the origin of flavor. The reason for the existence of three generations of fermions and for their hierarchical pattern of masses and mixing angles is, at present, not understood. The flavor physics of the third generation has been particularly mysterious. The smallness of the third generation mixing angles, and the huge hierarchy between the top and bottom quark masses have lead some to speculate that the third generation may be fundamentally different from the other two. Recent experimental results have also helped to motivate such speculation. There are a number of small discrepancies between the current experimental data and the expectations of the Standard Model concerning properties of the b-quark. The observed B-meson semileptonic branching ratio is much lower than the spectator parton model prediction, and the charm multiplicity in the decay products is also low, in both cases by roughly 20% [1]. Another possible anomaly is the high value of the $Z \to b\bar{b}$ width observed at LEP, though in this case the discrepancy with the Standard Model prediction is much smaller. Whether or not these are signs of new physics or merely systematic errors is subject to debate [2, 3]. Nevertheless, it is natural to question whether there are models that can explain the observed pattern of discrepancies, while remaining consistent with all the other relevant experimental constraints.

In this paper, we consider a model based on the gauge group $SU(3)_1 \times SU(3)_2 \times SU(3)_3 \times SU(2)_L \times U(1)_Y$. Quarks belonging to generation x transform as triplets under $SU(3)_x$, but as singlets under the other two SU(3)'s. We assume that $SU(3)_1 \times SU(3)_2$ breaks to its diagonal subgroup $SU(3)_{1,2}$ at some high scale Λ_H, and that $SU(3)_{1,2} \times SU(3)_3$ breaks to its diagonal subgroup, ordinary QCD, at a lower scale Λ_L. As we will see, the effective theory below Λ_L is simply the Standard Model with additional massive color octet gauge bosons, G_H, that couple preferentially to the third generation quarks. We will show that there are two regions of the parameter space of the model that are consistent with the constraints from the top quark production cross section, from collider searches for new particles decaying to dijets, and from flavor changing neutral current (FCNC) processes. In the latter case, we use the approach of Froggatt and Nielsen [4] to construct mass matrices that lead

to a natural suppression of the neutral flavor changing $\overline{q}G_H q$ couplings that arise at tree-level in the model. We show that it is possible within both of these allowed regions to obtain corrections to the nonleptonic B-decay widths that can reconcile the spectator parton model predictions for the semileptonic branching ratio and the average charm multiplicity per decay with the measured values. We also can obtain a correction to the $Z \to b\overline{b}$ width that reconciles the Standard Model expectation with the value observed at LEP, but in a different region of the parameter space. In the supersymmetric version of our model, however, we can obtain all three effects simultaneously. As a consequence of the new contribution to the $Z \to b\overline{b}$ width, the value of $\alpha_s(m_Z)$ extracted from $\Gamma(Z \to \text{hadrons})$ is reduced. This shift is sufficient to reconcile the LEP value of α_s with the measurements made at lower energies [3].

We should point out that the idea of introducing different gauge groups for each generation has appeared in various forms throughout the literature. However, most of the early references do not focus on the detailed phenomenology of the models [5], while the more recent references consider different $\mathrm{SU}(2)_L$s rather than SU(3)s to explain a now nonexistent anomaly in τ decay [6]. Our work is also similar in some respects to the recent literature on the phenomenology of topcolor models, which also involve additional massive color octet bosons [7]. In contrast to these references, we focus on the problem of constructing realistic mass matrices and the associated flavor physics. Since it is our purpose here to explore the anomalies described above, rather than to explain electroweak symmetry breaking through top condensation, we do not restrict ourselves to the case where the $\overline{q}G_H q$ coupling attains its critical value. In the strong-coupling limit of our model, we consider the possibility that the third generation quarks may become composite, in a way similar to the Abbott-Farhi model [8], without any condensation at all.

The paper is organized as follows. In Section 2, we present both the non-supersymmetric and supersymmetric versions of our model, and discuss the specific structure of the fermion mass matrices. The latter is crucial in determining the constraints from flavor-changing processes that we present in Sections 3 and 4. In Section 3 we identify the allowed parameter space of our model, and show that we can reproduce the value of R_b measured at LEP within the two allowed regions. In Section 4, we consider the $\Delta B = 1$

and $\Delta B = 2$ operators that result from a slightly more complicated form of the down-quark mass matrix. We show that the new $\Delta B = 1$ operators can reduce both the B-meson semileptonic branching ratio B_{SL} and the average charm multiplicity per decay n_c enough to reconcile the experimental data with the spectator parton model predictions. We show that the strong constraints from $b \to s\gamma$ in the non-supersymmetric version of the model only allow us to account for R_b and the B decay anomalies in different regions of the allowed parameter space. However, in the supersymmetric version, the $b \to s\gamma$ branching fraction is suppressed, allowing us to explain R_b, B_{SL} and n_c simultaneously. In Section 5 we consider what may happen in the confining phase of the color SU(3) corresponding to the third family, and argue that the bottom and top quarks may become composite. In the final section we summarize our conclusions.

2 The Model

We assume that the color gauge group $SU(3)_1 \times SU(3)_2 \times SU(3)_3$ is broken to $SU(3)_{1,2} \times SU(3)_3$ at some high scale $\Lambda_H \gtrsim \mathcal{O}(100)$ TeV by the vacuum expectation value (vev) of a Higgs boson $\Phi_{1,2}$ transforming as a $(\mathbf{3},\mathbf{3}^*,\mathbf{1})$. In the effective theory below Λ_H, the first and second generation fields have color charges under $SU(3)_{1,2}$ and the third generation fields under $SU(3)_3$. The group $SU(3)_{1,2} \times SU(3)_3$ is broken to its diagonal subgroup, $SU(3)_c$, at a much lower scale Λ_L by the vev of a Higgs boson $\Phi_{2,3}$ transforming as $(\mathbf{1},\mathbf{3},\mathbf{3}^*)$ under the original color group. The QCD coupling g_s is related to the couplings $g_{1,2}$ and g_3 by

$$\frac{1}{g_s^2} = \frac{1}{g_{1,2}^2} + \frac{1}{g_3^2}, \tag{1}$$

and thus we use the parameterization

$$g_{1,2} = \frac{g_s}{\cos\theta}, \tag{2}$$

$$g_3 = \frac{g_s}{\sin\theta}. \tag{3}$$

The last stage of symmetry breaking leaves a color-octet vector boson G_H with mass $M \sim g_s\Lambda_L/(\sin\theta\cos\theta)$ and with the following coupling to the

quarks:

$$\mathcal{L} = g_s G_H^{\mu a}(\bar{u}', \bar{c}', \bar{t}')\gamma_\mu T^a \begin{pmatrix} \tan\theta & 0 & 0 \\ 0 & \tan\theta & 0 \\ 0 & 0 & -\cot\theta \end{pmatrix} \begin{pmatrix} u' \\ c' \\ t' \end{pmatrix} + \text{down-sector} \ . \tag{4}$$

Here, the T^a are $SU(3)$ generators and the primed quark fields denote interaction eigenstates, which differ from the mass eigenstates in general. The symmetry breaking also leaves a color-octet scalar boson in the low-energy theory. The Higgs field $\Phi_{2,3}$ contains two color-octets under the diagonal $\mathrm{SU}(3)_c$; one of them is eaten by the vector boson G_H, while the other remains as a physical scalar multiplet.

The hierarchy of scales in the model is rendered natural through supersymmetry. The model can be easily supersymmetrized by introducing Higgs chiral superfields $\Phi_{2,3}$ transforming as $(\mathbf{1},\mathbf{3},\mathbf{3}^*)$ and $\Phi'_{2,3}$ as $(\mathbf{1},\mathbf{3}^*,\mathbf{3})$. The most general superpotential below the scale Λ_H is

$$W = \mu \mathrm{Tr}\Phi\Phi' + h\det\Phi + h'\det\Phi', \tag{5}$$

with a mass parameter μ, and coupling constants h, h'. It is amusing to note that $\det\Phi$ is a renormalizable interaction only for the $\mathrm{SU}(3)\times\mathrm{SU}(3)$ case. One can easily verify that this superpotential allows a desired minimum

$$\Phi = v \begin{pmatrix} 1 & & \\ & 1 & \\ & & 1 \end{pmatrix}, \qquad \Phi' = v' \begin{pmatrix} 1 & & \\ & 1 & \\ & & 1 \end{pmatrix}, \tag{6}$$

where

$$v = h^{-2/3}h'^{-1/3}\mu, \qquad v' = h^{-1/3}h'^{-2/3}\mu. \tag{7}$$

A color-octet supermultiplet is absorbed into the heavy vector multiplet, leaving two singlet chiral supermultiplets and one color-octet chiral supermultiplet. Hereafter, we will only refer explicitly to the supersymmetric generalization of the model when the superparticle content has a significant impact on the model's phenomenology.

Given the gauge symmetry of the full theory it is clear that we can only generate diagonal entries in the quark mass matrices. In order to generate realistic Cabibbo–Kobayashi–Maskawa (CKM) mixings, however, we require

off-diagonal entries in the basis of the interaction eigenstates as well. The way we can generate these off-diagonal components is through the exchange of heavy vector-like quarks [4]. We introduce a minimal set of vector-like quarks, U, C and D, which have the same quantum numbers as the ordinary right-handed quarks u_R, c_R, and d_R. Without a loss of generality, we can choose a basis where the invariant Dirac mass terms exist only for the U, C, and D fields and in which there is no mass mixing terms between U and u_R, etc. Given the Higgs representations described earlier, the most general set of Yukawa couplings involving the vector-like quarks is given by

$$\begin{aligned}\mathcal{L} = \bar{u}'_R\Phi_{1,2}C + \bar{U}\Phi_{1,2}c'_R + \bar{C}\Phi_{2,3}t'_R + \bar{D}\Phi_{1,2}s'_R \\ +\bar{Q}_1HD + \bar{Q}_1\tilde{H}U + \bar{Q}_2\tilde{H}C + h.c.,\end{aligned} \tag{8}$$

where H is the Higgs doublet of the minimal Standard Model, and $\tilde{H} = i\sigma_2 H^*$. It is straightforward to identify which Φ has to be replaced by Φ'^* in the supersymmetric case; H and $\tilde{H}$ must be replaced by H_1 and H_2 of the Minimal Supersymmetric Standard Model (MSSM) as well. After integrating out the vector-like quarks and replacing the Higgs fields $\Phi_{1,2}$, $\Phi_{2,3}$ and H by their respective vacuum expectation values, we obtain the following effective mass terms

$$\mathcal{L} \;=\; (\bar{u}'_L, \bar{c}'_L, \bar{t}'_L)M_u \begin{pmatrix} u'_R \\ c'_R \\ t'_R \end{pmatrix} + (\bar{d}'_L, \bar{s}'_L, \bar{b}'_L)M_d \begin{pmatrix} d'_R \\ s'_R \\ b'_R \end{pmatrix} + h.c., \tag{9}$$

where the mass matrices have the form

$$M_u = \begin{pmatrix} * & * & 0 \\ * & * & * \\ 0 & 0 & * \end{pmatrix}, \qquad M_d = \begin{pmatrix} * & * & 0 \\ 0 & * & 0 \\ 0 & 0 & * \end{pmatrix}. \tag{10}$$

Here each asterisk indicates a nonvanishing entry. By an appropriate choice of the vector-like quark masses and Yukawa couplings, we can obtain the following hierarchical form of the quark mass matrices without any fine-tuning of parameters

$$M_u \;\simeq\; \begin{pmatrix} m_u & m_c\lambda(\rho - i\eta) & 0 \\ \mathcal{O}(m_c\lambda^2) & m_c & m_tA\lambda^2 \\ 0 & 0 & m_t \end{pmatrix}, \tag{11}$$

$$M_d \simeq \begin{pmatrix} m_d & m_s\lambda & 0 \\ 0 & m_s & 0 \\ 0 & 0 & m_b \end{pmatrix}, \tag{12}$$

where we have written our result in terms of the Wolfenstein parameterization of the CKM matrix. The (2,1) entry in M_u does not give us a physically significant effect since it can be eliminated by a rotation on u_R and c_R below the scale Λ_H. [‡] Note that all masses and mixing parameters of the minimal Standard Model appear in the mass matrices above, and it is straightforward to check that they reproduce the correct form of the CKM matrix.[§] In fact, we can even drop the (2,1) entry completely, and still reproduce the correct CKM matrix.

One of our primary interests, however, is to consider the effects of our model on B-physics. Even though the mass matrices that we have constructed can perfectly reproduce the CKM matrix, they do not at the moment have any effect on B-physics because the first two generations are decoupled from the third in M_d; when we go to the mass eigenstate basis, we do not generate any new $\Delta B = 1$ operators via G_H exchange. Therefore, we introduce an additional vector-like quark B that has the same quantum numbers as b_R. The new Yukawa couplings involving the B field are given by

$$\Delta\mathcal{L} = \bar{s}'_R \Phi_{2,3} B + \bar{Q}_3 H B. \tag{13}$$

After integrating out the B field, we obtain a single new entry in the down-quark mass matrix, which we assume is of the order $m_b\lambda$ or less. Thus,

$$M_d \simeq \begin{pmatrix} m_d & m_s\lambda & 0 \\ 0 & m_s & 0 \\ 0 & m_b\lambda\xi & m_b \end{pmatrix}, \tag{14}$$

where $|\xi| \lesssim \mathcal{O}(1)$ is a new complex parameter.

[‡]This rotation leads to D^0-$\bar{D}^0$ mixing by the exchange of yet another color-octet vector boson coming from the breaking $SU(3)_1 \times SU(3)_2 \to SU(3)_{1,2}$. However, we assume that this breaking scale is very high $> \mathcal{O}(100)$ TeV to evade constraints from flavor-changing neutral currents processes.

[§]Therefore, the form of the mass matrix is not a *predictive* ansatz despite an interesting texture.

It is important to note that the mass matrices we have constructed not only reproduce the correct CKM matrix (despite their many zeros) but they also lead to relatively small FCNC effects from G_H exchange, as we will see in the next two sections. In addition, our form of the mass matrices have the nice feature that Cabbibo mixing is generated in the down-sector while V_{cb} is generated in the up-sector. This is preferred from the point of view of model building, since it leaves open the possibility of explaining the famous relation $\lambda \simeq \sqrt{m_d/m_s}$, and perhaps also $V_{cb} \simeq \sqrt{m_c/m_t}$. It is an interesting direction for future research to see whether it is possible to construct a realistic and predictive model within this framework, though we do not pursue this issue further here.

3 Parameter Space

In Figure 1 we show the allowed region of the M-$\cot\theta$ plane. The s-channel G_H exchange diagram can contribute significantly to the $t\bar{t}$ production cross section. We have adopted the central value of the $t\bar{t}$ cross section expected in the Standard Model from the next-to-leading order calculation by Laenen *et al.*[9], and have computed the shift of the production cross section in the $q\bar{q}$ channel expected in our model, including interference effects. The partonic cross section in the $q\bar{q}$ channel is given by

$$\hat{\sigma}(q\bar{q} \to t\bar{t}) = \frac{8\pi}{27}\alpha_s^2 \frac{1}{\hat{s}}\sqrt{1-\frac{4m_t^2}{\hat{s}}}\left[1+\frac{2m_t^2}{\hat{s}}\right] R \tag{15}$$

where $\hat{s}$ is the parton center of mass energy squared, and R is given by

$$R \equiv \frac{M^2(M^2+\Gamma^2)}{(\hat{s}-M^2)^2+M^2\Gamma^2} \tag{16}$$

The G_H width Γ is given by $\alpha_s M(4\tan^2\theta + \cot^2\theta)/6$, for decay to 5 light flavors, for example. We use the MRS D- structure functions in computing the total $q\bar{q}$ cross section, to be consistent with Ref [9] , and have assumed a K-factor of 1.2 to take into account next-to-leading-order effects. ¶ We require the total cross section to be within the 95% confidence level bounds of the

¶In fact, Laenen *et al.* use MRS D-' structure functions, but the difference is negligible for $t\bar{t}$ production.

value observed by CDF, $\sigma(t\bar{t}) = 6.8^{+3.6}_{-2.4}$ pb, for $m_t = 176 \pm 13$ GeV[10]. Because of the small statistics, the experimental errors are not exactly gaussian and there is a correlation between the errors in $\sigma(t\bar{t})$ and m_t. Unfortunately, the CDF paper [10] does not show the variation of χ^2 over an extended range of m_t, nor the dependence of the efficiency on m_t. Thus, we have no way to determine the 95% confidence level bound rigorously. We simply double the error bar on the CDF cross section to obtain an allowed range, 2–14 pb, for m_t between 150–202 GeV. Also, we do not take the correlation of the errors into account, and vary both $\sigma(t\bar{t})$ and m_t within the above ranges independently.[‖] We assumed a theoretical uncertainty in the central value of the Standard Model $t\bar{t}$ cross section that follows from varying the renormalization scale between $m_t/2$ and $2m_t$. The excluded region lies within the oval area between ~400 and ~800 GeV.

The dashed line in Figure 1 shows the bounds on new particles decaying to dijets at the 95% confidence level, from both UA1 [11] (between 200 and 300 GeV) and CDF [12] (between 200 and 850 GeV). The G_H decays to quark-antiquark pairs, like the more familiar axigluon, but its coupling to light quarks is suppressed by a relative factor of $1/\cot\theta$. Thus, given the published bounds on the axigluon production cross section, we can determine the value of $\cot\theta$ necessary to suppress the G_H cross section until it is below the experimental bound. From this, we conclude that the region below the dashed line is excluded. Note that the older UA1 bounds are more stringent below ~250 GeV due to higher statistics at smaller values of $\hat{s}$.

We also show the region allowed by the $Z \to b\bar{b}$ width measured at LEP. The new contribution to the parameter $R_b \equiv \Gamma(Z \to b\bar{b})/\Gamma(Z \to \text{hadrons})$ is given by

$$\frac{\Delta R_b}{R_b} = \frac{\frac{2}{3\pi}\alpha_s(\cot^2\theta - \tan^2\theta)(1 - R_b)F(M, M_Z)}{1 + \frac{2}{3\pi}\alpha_s\left[\tan^2\theta + (\cot^2\theta - \tan^2\theta)R_b\right]F(M, M_Z)} \tag{17}$$

where the function F is provided in Appendix A. Note that there is another contribution in the supersymmetric version of the model which involves the

[‖]Even though this "rectangular" treatment of the errors correspond to $(95\%)^2 = 90$ % confidence level, the final bound is determined by the corners of the rectangle, and hence correspond to 98 % confidence level in the (uncorrelated) Gaussian case. The true confidence level depends on both the correlation and non-Gaussian nature of the errors. Therefore, the excluded region in our figure should only be thought of as an approximate bound.

superpartners of the G_H-boson and the bottom quark. However, this diagram is roughly one order of magnitude smaller than the result in (17) [13].** Again we require that the Standard Model value of R_b plus the contribution given above remain within the 95% confidence level bound of the value measured at LEP, 0.2210±0.0029 [1]. The dotdashed line indicates the experimental central value, while the solid lines put an upper and lower bound on $\cot\theta$. Since there is a small discrepancy between the measured value from the Standard Model prediction, the central value lies away from the line $\cot\theta = 1$ where the effect vanishes. †† Note that the analogous quantity defined for charm quarks, R_c, is reduced in this model if $\cot\theta > 1$:

$$\frac{\Delta R_c}{R_c} = -\frac{R_b}{1-R_b}\frac{\Delta R_b}{R_b}. \tag{18}$$

Thus, when we account for the central value of R_b observed at LEP, we also obtain an -0.7% shift in R_c, which is completely negligible compared to the experimental error, $R_c = 0.171 \pm 0.020$ [1]. Other Z-pole observables do not give us any further constraints. For instance, the forward-backward and polarization asymmetries in $Z \to b\bar{b}$ are unaffected in our model because the G_H couples equally to left- and right-handed quarks.

Finally, we show the region excluded by flavor changing neutral current bounds in the case where the parameter $\xi = 0$. The case of nonvanishing ξ will be discussed together with the associated B physics in the next section. Given the minimal ($\xi = 0$) form of the mass matrices described in Section 2, there is no constraint from the down-sector, and the largest flavor changing neutral current bound comes from the D^0-$\overline{D}^0$ mass splitting. The effect is given approximately by

$$\Delta m_D = \frac{2\pi}{9}\alpha_s \frac{\lambda^{10}A^4(\rho^2+\eta^2)}{M^2\sin^2\theta\cos^2\theta} B_D f_D^2 m_D \eta_{QCD} \tag{19}$$

**Of course there could be an effect from the ordinary particle content of the MSSM, but it is negligible unless both the top squark and the chargino masses are just beyond the LEP limits.

††In evaluating (17), we have taken $\alpha_s(m_Z) = 0.110$, as determined by lattice QCD, rather than the LEP value. This is because the observed enhancement in $Z \to b\bar{b}$ is roughly in a one to one correspondence with the high value of $\alpha_s(m_Z)$ observed at LEP. However, it does not change our figure significantly if we choose $\alpha_s(m_Z) = 0.120$ instead. If we had used the preliminary number $R_b = 0.2204 \pm 0.0020$ presented at Moriond, which is 2.4 σ off from the Standard Model prediction, the allowed range lies in a narrower band above $\cot\theta = 1$ everywhere, while the curve for the central value does not shift significantly.

where $f_D = 208 \pm 37$ is the D^0 decay constant as determined from a lattice QCD calculation [14], and $\eta_{QCD} \approx 0.58$ is the QCD correction from running the four-quark operator down from M_Z to m_D, using the conventions of Buras *et al.* [15]. [‡‡] We take $B_D(m_c) = 1$ in our numerical analysis. We require that (19) is less than the experimental upper bound $\Delta m_D < 1.32 \times 10^{-10}$ MeV to determine the excluded region of the parameter space. This is appropriate because the Standard Model contribution to D^0-$\overline{D^0}$ mixing is expected to be $\sim$ 5 orders of magnitude smaller than the current experimental limit [16]. The excluded region lies to the left of the parabolic solid line shown in Figure 1.

The exchange of the color-octet Higgs boson also contributes to flavor-changing processes, but with a much smaller effect. The $\bar{t}'_R c'_L \Phi_{2,3}$ coupling is of order $m_t A\lambda^2/\langle\Phi_{2,3}\rangle$, and the coupling to the mass eigenstates $\bar{c}_R u_L$ is suppressed by an additional factor of $A\lambda^2(m_c/m_t) \times \lambda(\rho - i\eta)$. Thus, the contribution to Δm_D from Higgs exchange is down by at least $(m_c/m_t)^2$ compared to (19). We also checked that the exotic decay modes $t \to cg$, $c\gamma$ and $c\bar{b}b$ are negligible compared to the Standard Model decay $t \to bW$.

Taking all the constraints into account, we see from Figure 1 that there are two allowed "windows", in our model's parameter space: one small region at approximately $M \approx 250$ GeV, and a somewhat larger region above $M \approx 600$ GeV. If we further require that the central experimental value of R_b from LEP has to be reproduced, we must take $\cot\theta \sim 2$ in the light window and $\cot\theta \sim 4$ in the heavy window.

4 B-physics

Using the $\xi = 0$ form of the down-quark mass matrix, we showed in the previous section that we could account for R_b within the two allowed regions of our model's parameter space. In this section, we will consider the effects of the nonminimal ($\xi \neq 0$) form of M_d on B-physics. The question we would like to address is whether we can also reduce the B-meson semileptonic branching ratio B_{SL} and the charm multiplicity per decay n_c through the additional

[‡‡]We consistently ignore the effects of running between $\mu = M$ and m_Z, since $\log(m_Z/m_b) \gg \log(M/m_Z)$ and $\alpha_s(\mu > m_Z) < \alpha_s(\mu < m_Z)$ as well.

$\Delta B = 1$ operators that are present when $\xi \neq 0$, without conflicting with the constraints from FCNC processes. We will argue that our results strongly favor the supersymmetric version of the model.

With $\xi \neq 0$, we generate the following effective $\Delta B = 1$ operator through the exchange of the G_H boson.

$$\mathcal{L}_{eff} = \frac{g_s^2}{M^2}\frac{\lambda\xi}{\cos^2\theta}\bar{b}_R\gamma^\mu T^a s_R(\bar{u}\gamma^\mu T^a u + \bar{d}\gamma^\mu T^a d + \bar{s}\gamma^\mu T^a s + \bar{c}\gamma^\mu T^a c), \quad (20)$$

Since this operator always has an s_R in the final state, the amplitude does not interfere with the Standard Model amplitude (which only involves s_L) providing that we neglect m_s compared to m_b. Therefore, we add the new decay amplitude incoherently to that of the Standard Model. The QCD running modifies the normalization of the operator from the weak scale to the scale m_b; we take this into account in our numerical analysis below.

We estimate the additional contributions to the B partial decay widths from the effective operator in (20) using the parton-level spectator quark approximation. We find

$$\Delta\Gamma_B = \frac{m_b^5}{192\pi^3}\frac{N_C^2-1}{16N_C}\left(\frac{g_s^2\lambda\xi}{M^2\cos^2\theta}\right)^2[3G(0) + G(4m_c^2/m_b^2)], \quad (21)$$

where the function G is defined by

$$G(y) = \frac{1}{16}\sqrt{1-y}(16-40y+18y^2-9y^3)+\frac{3}{32}(8-3y)y^3\ln\frac{1+\sqrt{1-y}}{1-\sqrt{1-y}}, \quad (22)$$

and is normalized such that $G(0) = 1$.

As we described earlier, the current experimental data suggests that both the B semileptonic branching ratio B_{SL}, and the charm multiplicity per B decay n_c, are lower than the Standard Model expectations. Notice that decays via the operator (20) increase the total decay rate without affecting the semileptonic mode, and hence B_{SL} decreases. This operator also reduces n_c since it contributes to the $sq\bar{q}$ final state, which involves charm quarks only part of the time. We list the effects on B_{SL} and n_c for various choices of the parameters in Table. 1. The effect of G_H exchange is described by the parameter Δ, defined by

$$\Delta = \left(\frac{750\ \text{GeV}}{M}\right)^4\frac{\xi^2}{\cos^4\theta}. \quad (23)$$

masses	heavy		experiment
$\alpha_s(m_Z)$	0.105	0.115	
B_{SL}	$15.4(1-0.22\Delta)$	$12.7(1-0.28\Delta)$	10.6 ± 0.3 [18]
n_c	$1.09(1-0.21\Delta)$	$1.09(1-0.25\Delta)$	$1.08 \pm .06$ [20]

Table 1: Effect of G_H exchange on B-decay for the choice of "heavy" masses, $m_c = 1.7$ GeV and $m_b = 5.0$ GeV. The renormalization scale of the Standard Model operator is chosen at $\mu = m_b$.

masses	light		experiment
$\alpha_s(m_Z)$	0.105	0.115	
B_{SL}	$13.2(1-0.16\Delta)$	$12.7(1-0.20\Delta)$	10.6 ± 0.3 [18]
n_c	$1.21(1-0.13\Delta)$	$1.21(1-0.16\Delta)$	$1.08 \pm .06$ [20]

Table 2: Effect of G_H exchange on B-decay for the choice of "light" masses, $m_c = 1.2$ GeV and $m_b = 4.6$ GeV. The renormalization scale of the Standard Model operator is chosen at $\mu = m_b$.

We used the Standard Model predictions quoted in Ref. [18] with the renormalization scale $\mu = m_b$. For $\mu = m_b/2$, B_{SL} decrease by only 4%, while n_c does not change at all. The "heavy" case corresponds to $m_c = 1.7$ GeV, $m_b = 5.0$ GeV, and the "light" case to $m_c = 1.2$ GeV, $m_b = 4.6$ GeV. QCD renormalization effects were taken into account by numerically solving the renormalization group equation using the anomalous dimension matrix given in Ref. [19]. For the "heavy " quark masses it is difficult to reproduce the experimental values for any choice of Δ. However, one must keep in mind that the value of B_{SL} corresponding to the "heavy" quark masses is very far from the experimental data for $\Delta = 0$, indicating a more serious problem from the beginning. For "light" quark masses the discrepancy with the Standard Model predictions are $\sim 20\%$ for both B_{SL} and n_c, and we can easily obtain these shifts by an appropriate choice of the mixing parameter ξ, providing we do not exceed the bounds on other flavor changing processes, as we describe below.

Now that we have introduced mixing between b_R and s_R, we must also consider the constraints from the other FCNC processes associated with a nonvanishing value of ξ. We found that the most stringent constraint comes

from the contribution to B^0-$\overline{B}^0$ mixing from the operator

$$\mathcal{L} = \frac{1}{2}\left(\frac{g_s}{M\sin\theta\cos\theta}U_{31}^{d_R}\right)^2 \bar{b}_R\gamma^\mu T^a d_R \bar{b}_R\gamma_\mu T^a d_R, \tag{24}$$

Here, U^{d_R} is the rotation matrix acting on the right-handed down-type quarks, and $U_{31}^{d_R} \simeq \lambda\xi(\lambda m_d/m_s) \simeq \lambda^4\xi$ is the mixing angle between b_R and d_R. The renormalization of this operator down to the scale m_b gives us the correction factor $\eta_{QCD} \simeq 0.55$, again using the definition of η_{QCD} given in Ref [15]. The contribution to the mass splitting is then given by

$$\Delta m_B|_{G_H} = \frac{2\pi}{9}\alpha_s\left(\frac{\lambda^4\xi}{M\sin\theta\cos\theta}\right)^2 f_B^2 B m_B^2 \eta_{QCD}\ , \tag{25}$$

where $Bf_B^2 = (1.0 \pm 0.2)(180 \pm 50\ \text{MeV})^2$, based on recent lattice estimates [17]. As before, we obtain much smaller effects from octet Higgs exchange. The sum of the Standard Model contribution $\Delta m_B|_{SM}$ and $\Delta m_B|_{G_H}$ shown above should give us the experimental value

$$\left|\Delta m_B|_{SM} + \Delta m_B|_{G_H}\right| = \Delta m_B|_{expt} \tag{26}$$

where $\Delta m_B|_{expt} = 3.357 \times 10^{-13}$ GeV. However, the Standard Model prediction depends sensitively on the choice of V_{td}. If we fix $m_t = 176$ GeV and $Bf_B^2 = (180\ \text{MeV})^2$, then $\Delta m_B|_{SM}$ can range between (0.16–2.50) $\Delta m_B|_{expt}$ [17] if we allow V_{td} to vary within the 90% C.L. range allowed by CKM unitarity $V_{td} = 0.004$–0.015 [1]. Since the phase of the parameter ξ is arbitrary, we obtain the bound $\left|\Delta m_B|_{G_H}\right| < 3.5\ \Delta m_B|_{expt}$, and hence

$$M < \frac{3.11\ \text{TeV}}{\sqrt{\Delta}}\frac{1}{\cot\theta}\ . \tag{27}$$

Since we have used the 90% C.L. upper bound on V_{td} in deriving this expression while keeping m_t and Bf_B^2 fixed at their central values, it follows that the actual 95% C.L. bound is weaker than the one given in (27). We use this strict bound to demonstrate that even with conservative assumptions there exists an allowed range in the parameter space of the model when $\Delta \approx 1$. If we choose $\Delta = 1$, so that we can account for a 20% reduction in B_{SL} and n_c, then we must also be below the dashed line shown in Figure 2 to evade the B-$\overline{B}$ mixing constraint given by (27). Thus far, we see that both in the

light and heavy windows, we can explain the anomalies in B_{SL}, n_c, and R_b simultaneously.

The only other potentially significant FCNC constraint that depends on the parameter ξ and that may alter our conclusions is the $b \to s\gamma$ branching fraction. Note that *all* of the flavor-changing processes that we have considered until now have received contributions at tree-level in our model, while the $b \to s\gamma$ width receives contributions at the one-loop level only. This point is significant because the supersymmetric particle content of our model can now have a dramatic effect on the result.

Let us consider the upper bound that we can place on $\cot\theta$ from the $b \to s\gamma$ branching fraction. The most important contributions to the amplitude for $\cot\theta > 1$ come from the Feynman diagrams proportional to $1/\sin^2\theta$, shown in Figure 3. If we first consider the non-supersymmetric case, the entire nonstandard contribution to the inclusive branching fraction comes from the first diagram. If we compare this to the difference between the CLEO upper bound, 4.2×10^{-4} [22] and the Standard Model expectation, 1.9 ± 0.54 [23], and require agreement within two standard deviations, then we obtain the constraint

$$\cot\theta < 1.7/\sqrt[4]{\Delta} \tag{28}$$

If we require $\Delta = 1$ to explain the B-decay anomalies, then we see that (28) forces us to live in the lower right handed corner of the allowed region in Figure 2, where we cannot simultaneously explain the central value of R_b.

However, the situation changes dramatically in the supersymmetric case. It is well known that the $b \to s\gamma$ branching fraction vanishes identically in the limit of exact supersymmetry [21]. Thus, the new contribution to $b \to s\gamma$ in our model not only depends on M and $\cot\theta$, but also on the soft-SUSY breaking masses and couplings. In addition to the diagram involving ordinary particles, there are a number of other diagrams that involve the exchange of the left- and right-handed b-squarks, ($\tilde{b}_L$, $\tilde{b}_R$) and the fermionic partners of the transverse and longitudinal components of the G_H-boson (ψ, χ). The new diagrams tend to cancel the first one. An exact result for these diagrams is provided in Appendix B. If we assume that the soft SUSY-breaking masses defined in Appendix B are around 100 GeV, temporarily ignore $\tilde{b}_L$-$\tilde{b}_R$ mixing effects (i.e. ignore the fourth diagram), and compare the total result for the

inclusive branching fraction to the CLEO upper bound, we now find

$$\begin{aligned} \cot\theta &< 3.2/\sqrt[4]{\Delta} \quad (M = 250 \text{ GeV}), \\ \cot\theta &< 5.5/\sqrt[4]{\Delta} \quad (M = 640 \text{ GeV}). \end{aligned} \tag{29}$$

correspoding to bound (a) in Figure 2. In this case we do not exclude the interesting regions of our parameter space when $\Delta = 1$. We show the regions excluded for $\Delta = 1$ and for various choices of the SUSY breaking parameters in Figure 2. Note that we have not included the QCD running effects in these bounds since the relevant anomalous dimension matrix is not available in the literature. While this effect may give an important correction to our estimates above, our conclusions will not change once we take into account the strong dependence of our results on the soft supersymmetry-breaking parameters. For example the running of the $b \to s\gamma$ operator itself results in a suppression in the amplitude by a factor of ~ 0.7, while the four-fermi operator Eq. (20) may feed into the $b \to s\gamma$ operator at the two-loop level and enhance the amplitude by a factor of 2 or 3. However, if we include the $\tilde{b}_L$-$\tilde{b}_R$ mixing in the fourth diagram, it is easy to obtain a suppression of approximately the same size without any real fine-tuning (*e.g.* the difference between bounds (b) and (c) in Figure 2). This is possible because we do not know the magnitude or phase of the soft SUSY-breaking parameter A. With $A \approx 100$ GeV, the bounds in (29) become

$$\begin{aligned} \cot\theta &< 3.8/\sqrt[4]{\Delta} \quad (M = 250 \text{ GeV}), \\ \cot\theta &< 8.6/\sqrt[4]{\Delta} \quad (M = 640 \text{ GeV}). \end{aligned} \tag{30}$$

While a complete study of this enlarged parameter space is beyond the scope of this paper, it is clear that the suppression of $b \to s\gamma$ in the supersymmetric case, as well as the additional parametric degrees of freedom prevent us from excluding additional regions of the M-$\cot\theta$ plane when $\Delta = 1$ (*c.f.* bound (d) in Figure 2). Thus, we can account for the observed value of R_b, and obtain a 20% reduction in B_{SL} and n_c simultaneously.

5 Confinement Phase of $SU(3)_3$

We have seen that it is possible to explain the anomalies in R_b, B_{SL} and n_c in both allowed regions of our model's parameter space. However, the

strong possibility that the lighter window ($M \approx 250$ GeV) may be ruled out in the near future by the improving bounds on new particles decaying to dijets makes the heavier region ($M \gtrsim 600$ GeV) worthy of further consideration. In order to reproduce the central value of R_b in this region would require that we take $\cot\theta \sim 4$, which implies a rather large $SU(3)_3$ gauge coupling. This leaves open the possibility of nontrivial nonperturbative dynamics. For example, if the dynamics of the third family in the limit of large g_3 is like the Nambu–Jona-Lasinio model, then we would expect chiral symmetry breaking at a critical coupling of $\cot\theta = \sqrt{\pi/(3\alpha_s)} \approx 3.4$, and a large dynamical mass for both the top and bottom quarks. This would not be phenomenologically acceptable. However, what actually happens in this limit depends on the nonperturbative dynamics and on the mass of the Higgs boson $\Phi_{2,3}$. In this section, we consider the possibility that the $\mathrm{SU}(3)_3$ gauge theory may be confining, and that the physical bottom and top quarks may be composite particles, bound states of the fundamental quark fields and the Higgs field $\Phi_{2,3}$. We will argue that the phenomenology of such a confining phase is the same as the Higgs phase we have described in the previous three sections, providing that the third family dynamics is similar to the Abbott–Farhi model [8].

Let us consider what happens if $g_3 \gg 1$ and $\mathrm{SU}(3)_3$ is confining. If $\Phi_{2,3}$ is much heavier than the scale at which g_3 becomes large, then $\Phi_{2,3}$ decouples from the dynamics and we expect spontaneous chiral symmetry breakdown, and a large dynamical mass for the third generation quarks. If $\Phi_{2,3}$ is lighter than the scale at which the $SU(3)_3$ coupling becomes strong, then complementarity [24] suggests that the resulting confinement phase should be smoothly connected to the Higgs phase described earlier in this paper. Thus, we expect the physical top and bottom quarks to become composites of the fundamental top and bottom quarks with the $\Phi_{2,3}$ boson. We identify physical composite top and bottom states, t_c and b_c, with the composite operators $(\Phi t)/\Lambda$ and $(\Phi b)/\Lambda$, where Λ is the compositeness scale. Note that these composite states transform as triplets under $SU(3)_{1,2}$ as desired. In this phase it is not necessary to have $\langle\bar{t}t\rangle$ or $\langle\bar{b}b\rangle$ condensates since the low-energy fermion content satisfies the 'tHooft anomaly matching conditions, as in the Abbott–Farhi model [8]. There is a ρ-like meson state in the confining phase composed of $t\bar{t}$, $b\bar{b}$ and $\Phi\Phi^*$ bound states, which corresponds to the G_H

boson of the Higgs phase. The composite top and bottom quarks would remain massless if it were not for the explicit chiral symmetry breaking effects of their associated Yukawa couplings, and hence the masses of the composite states are proportional to their Yukawa couplings as before.

All the phenomenological constraints that we have discussed also carry over smoothly to the confining picture. For example, let us consider the $q\bar{q} \to t\bar{t}$ cross section presented in Section 3. The only contribution to this process in the confining picture is s-channel gluon exchange, but now there is a form factor $F(q^2)$ at the gluon-$t_c\bar{t}_c$ vertex. Assuming vector-meson dominance, $F(q^2)$ is saturated by the exchange of the ρ-like meson (G_H), which mixes with the gluon. Since $F(q^2)$ should reduce to the form factor for a point-like interaction $F(q^2) \to 1$ in the $q^2 \to 0$ limit, it must be of the form

$$F(q^2) = \frac{-M^2 + iM\Gamma}{q^2 - M^2 + iM\Gamma} \tag{31}$$

for small q^2. Thus, the cross section computed in the confining phase has exactly the same dependence on M and Γ as the cross section we obtained from perturbative G_H exchange in the Higgs phase. We can also describe the phenomenology of the confining phase in terms of the same parameter space as the Higgs phase, providing that $q^2 \ll M^2$. The ρ-like meson does not couple to the light quarks directly, while the coupling to t_c and b_c is an unknown parameter that we can identify with $g_s \cot\theta$. Therefore, the correction to R_b involves the same combination of parameters as before. The dimension-five operators generated by the exchange of vector-like fermions induce mixing between elementary light quarks and composite third generation quarks, and the flavor off-diagonal coupling of the ρ-like meson is proportional to $g_s \cot\theta$, again consistent with the Higgs phase result in the limit $\cot\theta \to \infty$.

6 Conclusions

We have shown that the extension of the Standard Model presented in this paper can yield corrections to R_b, the B-meson semileptonic branching ratio and the charm multiplicity in B-decays, in a pattern roughly consistent with the experimental data. In the nonsupersymmetric version of the model, we can explain either the value of R_b, or the B-decay anomalies within the al-

lowed parameter space of our model, but not both simultaneously. This is a consequence of the strong upper bound on $\cot\theta$ that we obtain from the limit on $b \to s\gamma$, when we take $\Delta = 1$. However, the natural suppression of $b \to s\gamma$ in the supersymmetric version of the model allows for choices of the parameters that can account for R_b and the B-decay anomalies simultaneously. Because the massive color octet bosons in this model couple more strongly to third generation quarks, a natural way to test this idea is to search for a high mass peak in the $b\bar{b}$ dijet invariant mass distribution at hadron colliders. This may rule out the small allowed window that we found near $M \approx 250$ GeV in the near future.* At present it is interesting to note that the most recent search at CDF [12] for new particles decaying to dijets has found upward statistical fluctuations in the data near 250, 550, and 850 GeV [12]. While probably nothing more than coincidental, it is amusing to note that two of these masses fall within the two allowed regions in our model's parameter space. Finally, we have considered the limit in which the SU(3) associated with the third family quarks becomes confining, and argued that the bottom and top quarks may become composite objects without forming condensates, like the composite fermions of the Abbott-Farhi Model. We argued that the phenomenology of the confinement phase should be smoothly connected to that of the Higgs phase described in this paper. Thus, it is possible that third family compositeness effects may give us other nontrivial signatures of this model.

Acknowledgments

We thank JoAnne Hewett and Tom Rizzo for useful comments. *This work was supported by the Director, Office of Energy Research, Office of High Energy and Nuclear Physics, Division of High Energy Physics of the U.S. Department of Energy under Contract DE-AC03-76SF00098.*

A Appendix

The function $F(M, M_Z)$ defined in Eq. 17 is given by

$$F(M, M_Z) \equiv F_1 + F_2 \tag{32}$$

*A search is currently under way at CDF, but the data analysis has not yet been completed.

for $M < m_Z$ and

$$F(M, M_Z) \equiv F_2 \tag{33}$$

for $M > m_Z$, where

$$\begin{aligned} F_1 &= (1+\delta)^2\left[3\ln\delta + (\ln\delta)^2\right] + 5(1-\delta^2) - 2\delta\ln\delta \\ &\quad -2(1+\delta)^2\left[\ln(1+\delta)\ln\delta + \mathrm{Li}_2\left(\frac{1}{1+\delta}\right) - \mathrm{Li}_2\left(\frac{\delta}{1+\delta}\right)\right], \end{aligned} \tag{34}$$

$$\begin{aligned} F_2 &= -2\left\{\frac{7}{4} + \delta + (\delta + \frac{3}{2})\ln\delta \right. \\ &\quad \left. +(1+\delta)^2\left[\mathrm{Li}_2\left(\frac{\delta}{1+\delta}\right) + \frac{1}{2}\ln^2\left(\frac{\delta}{1+\delta}\right) - \frac{\pi^2}{6}\right]\right\}. \end{aligned} \tag{35}$$

Here $\mathrm{Li}_2(x) = -\int_0^x \frac{dt}{t}\ln(1-t)$ is the Spence function, and $\delta = M^2/m_Z^2$.

B Appendix

The effective operator yielding the largest contribution to to $b \to s\gamma$ for $\cot\theta > 1$ is given by

$$\frac{1}{36\pi^2}\frac{eg_s^2\lambda\xi}{\sin^2\theta}\frac{m_b}{M^2}\sum_i \frac{c_i}{2}\,\overline{s}_R\,\sigma^{\alpha\beta}F_{\alpha\beta}\,b_L \tag{36}$$

where $F_{\alpha\beta}$ is the photon field strength tensor, and the index i runs over the four classes of diagrams shown in Figure 3. We find to lowest order in the bottom quark mass:

$$c_1 = \frac{4}{3} \tag{37}$$

$$c_2 = -\sum_i \frac{U_{\psi i}U_{\chi i}M}{\mu_i}\left[\frac{1 - r_i^4 + 2r_i^2\ln(r_i^2)}{(1-r_i^2)^3}\right] \tag{38}$$

$$c_3 = -\sum_i \frac{U_{\psi i}U_{\psi i}^\dagger M^2}{\mu_i^2}\left[\frac{\frac{1}{6}p_i^6 - p_i^4 + \frac{1}{2}p_i^2 + p_i^2\ln(p_i^2) + \frac{1}{3}}{(1-p_i^2)^4}\right] \tag{39}$$

$$\begin{aligned} c_4 &= 2A\sum_i \frac{U_{\psi i}U_{\psi i}M^2}{\mu_i^3}\left[\frac{-4 + (1+p_i^2)(1+r_i^2)}{2(1-p_i^2)^2(1-r_i^2)^2}\right. \\ &\quad \left. -\frac{r_i^2}{(1-r_i^2)^3(r_i^2-p_i^2)}\ln r_i^2 - \frac{p_i^2}{(1-p_i^2)^3(p_i^2-r_i^2)}\ln p_i^2\right] \end{aligned} \tag{40}$$

where we have neglected terms of order m_b^2/M^2. Above the μ_i are the eigenvalues of the ψ-χ mass matrix

$$\begin{pmatrix} m_\psi & M \\ M & m_\chi \end{pmatrix} \tag{41}$$

where ψ is the superpartner of the the transverse component of the G_H, and χ is the superpartner of the would-be Nambu Goldstone boson in $\Phi_{2,3}$. Note that the off-diagonal entries are generated by the vacuum expectation value of $\Phi_{2,3}$, while the diagonal ones are SUSY breaking effects. U is the matrix that diagonalizes (41), $r_i = m_{\tilde{b}_L}/\mu_i$, and $p_i = m_{\tilde{b}_R}/\mu_i$. In the final diagram, Am_b parameterizes the $\tilde{b}_L$-$\tilde{b}_R$ mass squared mixing, where A is the trilinear soft SUSY breaking parameter.

References

[1] L. Montanet *et al.*, Particle Data Group, *Phys. Rev.* **D50**, 1173 (1994).

[2] A.L. Kagan, SLAC-PUB-6626, hep-ph/9409215.

[3] M. Shifman, TPI-MINN-94-42-T, hep-ph/9501222.

[4] C.D. Froggatt and H.B. Nielsen, *Nucl. Phys.* **B147**, 277 (1979).

[5] A. Salam, in *Proceedings of the European Physical Society International Conference on High Energy Physics*, Geneva, 1979, edited by A. Zichichi (CERN, Geneva, 1980), footnote 41 therein; S. Rajpoot, *Phys. Rev.* **D24**, 1890 (1981); X.-Y. Li and E. Ma, *Phys. Rev. Lett.* **47**, 1788 (1981); H. Georgi, *Nucl. Phys.* **B202**, 397 (1982);

[6] M. Fukugita, H. Murayama, K. Suehiro, and T. Yanagida, *Phys. Lett.* **B283**, 142 (1992); X.-Y. Li and E. Ma, *Phys. Rev.* **D46**, 1905 (1992); *J. Phys.* **G19**, 1265 (1993).

[7] C.T. Hill, *Phys. Lett.* **B266**, 419 (1991); C.T. Hill and X. Zhang, FERMILAB-PUB-94/231-T, hep-ph/9409315.

[8] L.F. Abbott and E. Farhi, *Phys. Lett.* **B101**, 69 (1981); *Nucl. Phys.* **B189**, 547 (1981);

[9] E. Laenen, J. Smith and W.L. van Neerven, *Phys. Lett.* **B321**, 254 (1994).

[10] CDF collabration, FERMILAB-PUB-95/022-E, hep-ex/9503002.

[11] C. Albajar *et al.*, UA1 collaboration, *Phys. Lett.* **B2-0**, 127 (1988).

[12] F. Abe *et al.*, CDF collaboration, hep-ex/9501001. Actually their earlier paper (*ibid.*, *Phys. Rev. Lett.* **71**, 2542 (1993)) quotes more stringent limits on the resonant excess cross section, but they assume isotropic decays of the resonance and hence an acceptance that is too optimistic.

[13] K. Hagiwara and H. Murayama, *Phys. Lett.* **B246**, 533 (1990).

[14] C.W. Benard, J.N. Labrenz, A. Soni, *Phys. Rev.* **D49**, 2536 (1994).

[15] A.J. Buras, M. Jamin, and P.H. Weisz, *Nucl. Phys.* **B347**, 491 (1990).

[16] H. Georgi, *Phys. Lett.* **B297**, 353 (1992); T. Ohl, G. Ricciardi, and E.H. Simmons, *Nucl. Phys.* **B403**, 605 (1993);

[17] R. Forty,CERN-PPE-94-154, Oct 1994, Review talk at Int. Conf. on High Energy Physics, Glasgow, Scotland, Jul 20-27, 1994.

[18] G. Altarelli and S. Petrarca, *Phys. Lett.* **B261**, 303 (1991).

[19] B. Grinstein, R. Springer and M.B. Wise, *Nucl. Phys.* **B339**, 269 (1990).

[20] F. Muheim, talk given at DPF '94, Alberquerque, New Mexico, August, 1994.

[21] S. Ferrara and E. Remiddi, *Phys. Lett.* **B53**, 347 (1974); R. Barbieri and G.F. Giudice, *Phys. Lett.* **B309**, 86 (1993)

[22] CLEO Collaboration (M.S. Alam, *et al.*) *Phys. Rev. Lett.* **74**, 2885 (1995).

[23] M. Ciuchini, *et al.*, *Phys. Lett.* **B334**, 137 (1994)

[24] G. 't Hooft, Cargèse Summer Institute Lectures (1979).

Figure Captions

Fig. 1. Allowed regions of the M-$\cot\theta$ plane, for $\xi = 0$. The region above (below) the upper (lower) solid line is excluded by R_b, the region below the dashed line is excluded by searches at UA1 and CDF for new particles decaying to dijets, the region inside the dashed "oval" is excluded by the $t\bar{t}$ production cross section, and the region to the left of the solid parabola is excluded by D-$\overline{D}$ mixing. The dotdashed line shows the central value for R_b measured at LEP.

Fig. 2. Allowed regions of the M-$\cot\theta$ plane, for excluded by B-$\overline{B}$ mixing, for the choice of Δ shown. The region above each dashed line is excluded by the $b \to s\gamma$ constraint for $\Delta = 1$, and for various choices of the soft SUSY breaking masses ($m_{\tilde{b}_R}$, $m_{\tilde{b}_L}$, m_ψ, m_χ, A). The dashed lines correspond to the following mass sets (in GeV): (a) (100,100,100,100,0), (b) (200,200,200,200,0), (c) (200,200,200,200,200), (d) (300,100,200,200,200). The non-supersymmetric result is also shown.

Fig. 3. Feynman diagrams proportional to $1/\sin^2\theta$ that contribute to $b \to s\gamma$. The numbering of the diagrams corresponds to the results presented in Appendix B.

Fig. 1

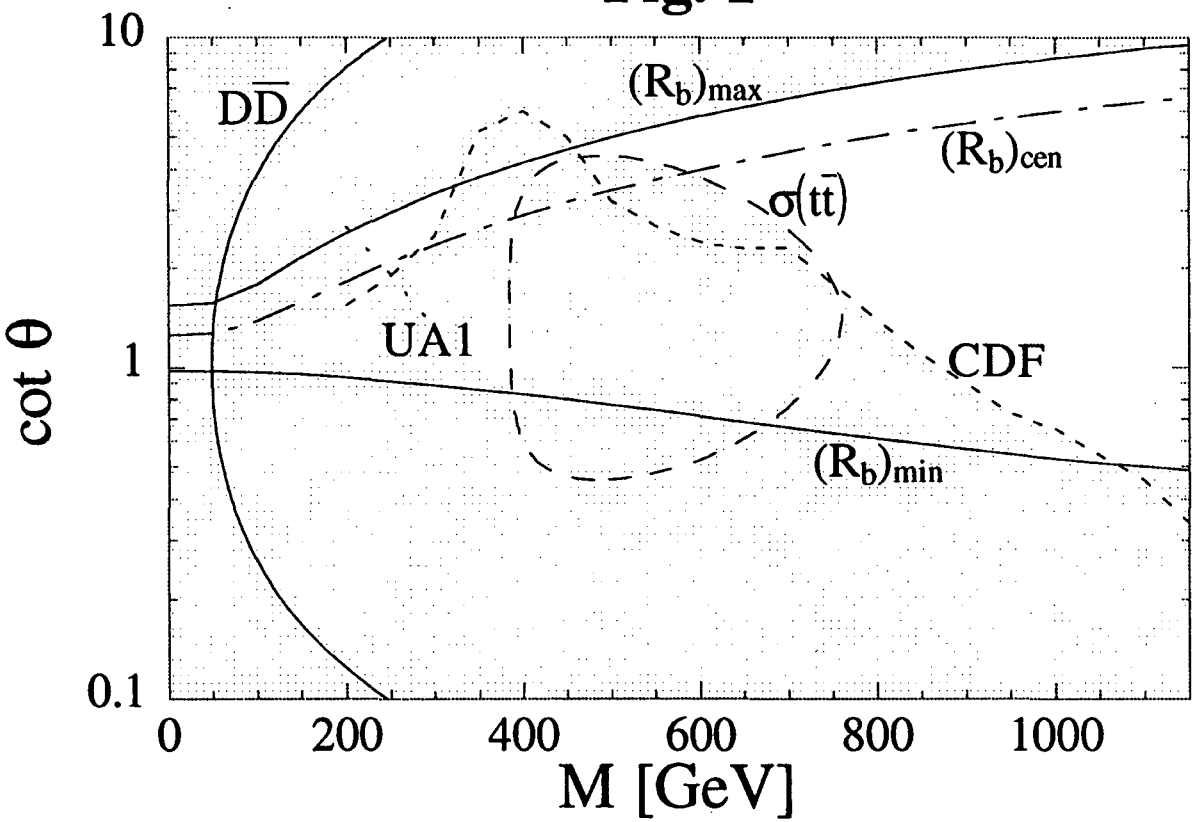
10
1
0.1
cot θ
0
200
400
600
800
1000
M [GeV]
DD̄
(R_b)_max
(R_b)_cen
σ(tt̄)
UA1
CDF
(R_b)_min

Fig. 2

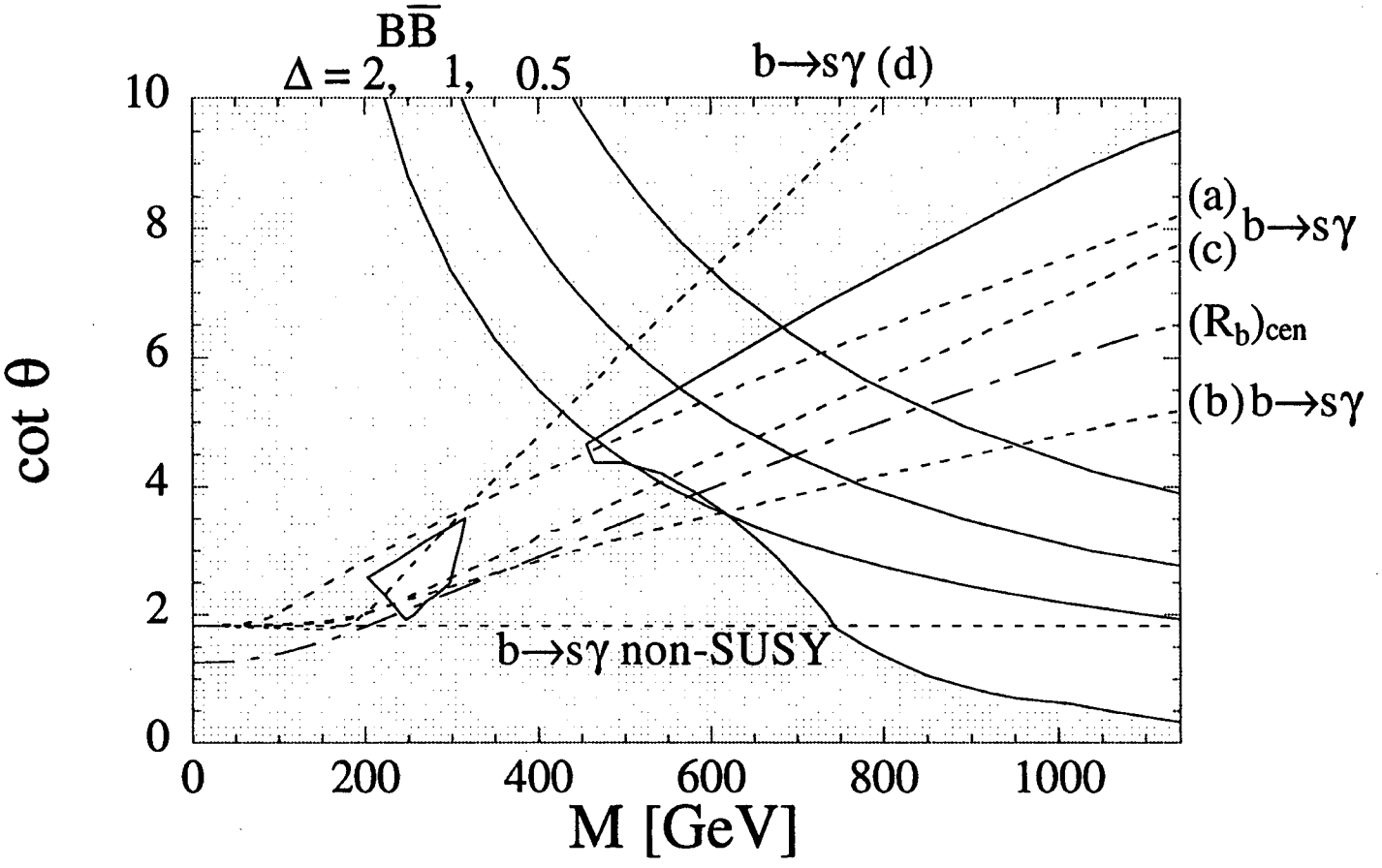
$B\overline{B}$
$\Delta = 2,\ 1,\ 0.5$
$b \to s\gamma$ (d)
(a)
(c)
$b \to s\gamma$
$(R_b)_{cen}$
(b) $b \to s\gamma$
$b \to s\gamma$ non-SUSY
cot θ
M [GeV]
0
2
4
6
8
10
0
200
400
600
800
1000

Fig. 3

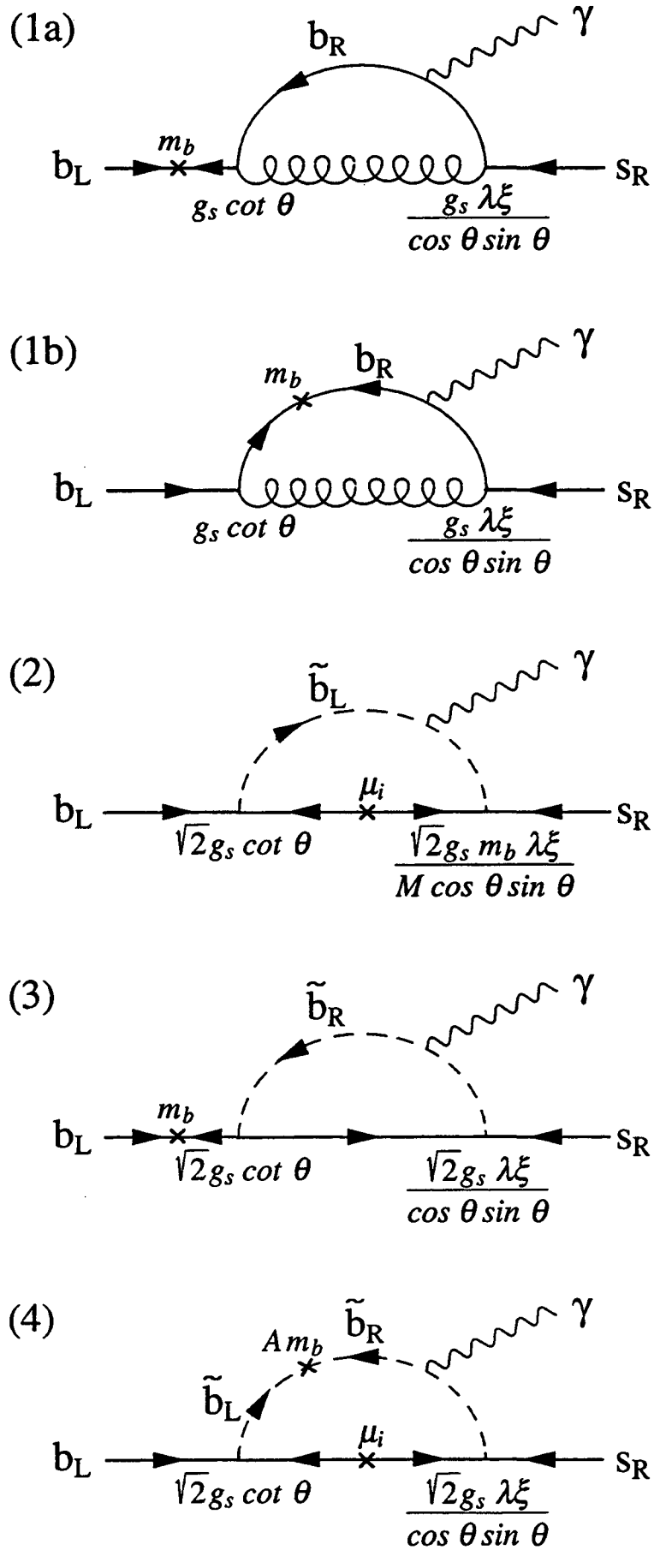
(1a)
b_R
γ
m_b
b_L
s_R
$g_s \cot\theta$
$\frac{g_s \lambda\xi}{\cos\theta \sin\theta}$
(1b)
m_b
b_R
γ
b_L
s_R
$g_s \cot\theta$
$\frac{g_s \lambda\xi}{\cos\theta \sin\theta}$
(2)
$\tilde{b}_L$
γ
μ_i
b_L
s_R
$\sqrt{2} g_s \cot\theta$
$\frac{\sqrt{2} g_s m_b \lambda\xi}{M \cos\theta \sin\theta}$
(3)
$\tilde{b}_R$
γ
m_b
b_L
s_R
$\sqrt{2} g_s \cot\theta$
$\frac{\sqrt{2} g_s \lambda\xi}{\cos\theta \sin\theta}$
(4)
$A m_b$
$\tilde{b}_R$
γ
$\tilde{b}_L$
μ_i
b_L
s_R
$\sqrt{2} g_s \cot\theta$
$\frac{\sqrt{2} g_s \lambda\xi}{\cos\theta \sin\theta}$

LAWRENCE BERKELEY LABORATORY
UNIVERSITY OF CALIFORNIA
TECHNICAL INFORMATION DEPARTMENT
BERKELEY, CALIFORNIA 94720